

Project information

Project full title	Connecting Russian and European Measures for Large-scale Research Infrastructures – plus
Project acronym	CREMLINplus
Grant agreement no.	871072
Instrument	Research and Innovation Action (RIA)
Duration	01/02/2020 – 31/01/2024
Website	www.cremlinplus.eu

Deliverable information

Deliverable no.	D6.2 (D54)
Deliverable title	Prototype of pulse compressor based on self-phase modulation
Deliverable responsible	IAP RAS
Related Work-Package/Task	WP6; Task 6.1
Type (e.g. Report; other)	Demonstrator
Author(s)	Efim Khazanov
Dissemination level	Public
Document Version	2
Date	17.01.2022
Download page	https://www.cremlinplus.eu/results/deliverables/

Document information

Version no.	Date	Author(s)	Comment
1	13.01.2022	Efim Khazanov	
2	17.01.2022	Efim Khazanov	

[Table of Contents].....

Introduction
Features of nonlinear compression
Experiments with the prototype
Conclusion
Research team



Prototype of pulse compressor based on self-phase modulation

Introduction

We have demonstrated compression of the input pulse of the laser PEARL with an energy of 18 J and pulse duration of about 60 fs to 10 fs after passage through a 4-mm thick KDP crystal and reflection at two chirped mirrors with sum dispersion -200 fs^2 . This outstanding result was obtained using the Compression after Compressor Approach (CafCA) also called Thin Film Compression or Post-compression. According to this approach, the pulse spectrum is broadened as a result of self-phase modulation (SPM) during propagation in a medium with Kerr nonlinearity and then compressed due to reflection from chirped mirrors (CM) with negative dispersion.

The idea to use cubic nonlinearity for SPM was known for quite a time but despite a huge number of works, pulses were compressed only with mJ energy, and the energy efficiency was less than 50%. In the recent years, quite a few experimental results were obtained, in which CafCA was successfully implemented for pulses with an energy of 1-18 J and energy efficiency close to 100%. An important impetus for these studies was the proposed and experimentally confirmed method of suppressing small-scale self-focusing even at large values of the B-integral

$$B = (2\pi/\lambda_0) L n_2 I_{in} \quad (1)$$

where n_2 and L are, respectively, the nonlinear index of refraction and the thickness of the nonlinear medium, $\lambda_0 = 2\pi c/\omega_0$ is the central wavelength in vacuum, and I_{in} is the input peak intensity. It was confirmed that large B-integral values enable a significant increase in the compression ratio. In our work aimed at the development of an SMP-based pulse compressor we experimentally studied the compression of an output pulse of the laser PEARL (PEtawatt pARametric Laser) by SMP in a KDP crystal in a wide range of B-integral values from 5 to 19 and compared the obtained results with the ones using silica. A substantial contribution to the present result was also made by the earlier demonstration of two-stage compression and the theoretical works on detailed numerical modeling and on expanding the capabilities of the technique aimed at simultaneous contrast enhancement.

Features of nonlinear compression

All the aspects of nonlinear compression (spectrum broadening, pulse shortening, and peak intensity increase) were considered as a function of two key parameters – the B-integral (1) and the dimensionless parameter of nonlinear medium dispersion D

$$D = L \frac{k_2}{T_F^2} \quad (2)$$

where T_F is the FWHM-duration of the input Fourier-transform-limited (FTL) Gaussian pulse. The parameters B and D characterize nonlinearity and dispersion and have a simple physical meaning: B is the ratio of the medium length L to the nonlinear length (the length at which a nonlinear phase equal to 1 is accumulated) and D is the ratio of L to the dispersion length $L_{d1} = T_F^2/k_2$. The KDP crystal at the wavelength $\lambda=910 \text{ nm}$ has a very small value of $k_2=11.3 \text{ fs}^2/\text{mm}$. Hereinafter, we use the Sellmeier equation. Moreover, k_2 reduces with growing λ and at $\lambda=985 \text{ nm}$ changes its sign. Consequently, not only group velocity dispersion k_2 but also the next, third-order dispersion (TOD) should be taken into account. For silica, the value of k_2 is much higher ($28 \text{ fs}^2/\text{mm}$). However, as will be shown below, at large B values TOD impact is still more significant.

With allowance for TOD, the laser pulse propagation in a medium with Kerr nonlinearity is described by the equation

$$\frac{\partial a}{\partial \xi} - \frac{i \cdot D}{2} \frac{\partial^2 a}{\partial \eta^2} + \frac{T}{6} \frac{\partial^3 a}{\partial \eta^3} = -iB \left(|a|^2 \cdot a - \frac{2 \cdot i}{\pi \cdot N} \frac{\partial}{\partial \eta} \left(|a|^2 \cdot a \right) \right) \quad (3)$$

where $\xi=z/L$, z is the longitudinal coordinate, L is the thickness of the plate, $\eta=(t-z/u)/T_F$, $\frac{1}{u} = \frac{\partial k(\omega)}{\partial \omega} \Big|_{\omega=\omega_0}$, $a=A/A_{10}$ is the complex amplitude of the field normalized to the value at the input boundary (A_{10}), $T=Lk_3/T_F^3$ is

the dimensionless parameter TOD, $k_3 = \frac{1}{2k_0} \frac{\partial^3 k(\omega)}{\partial \omega^3} \Big|_{\omega=\omega_0}$, $k(\omega)=n(\omega)\omega/c$ is the wave vector, $k_0=k(\omega_0)$,

$N=T_F/\tau$, and $\tau = 2\pi/\omega_0$ is the period of the optical field. Let at the input of the nonlinear medium there be a Gaussian FTL pulse



$$a(t, z = 0) = e^{-2 \ln(2) \frac{t^2}{T_F^2}} \quad (4)$$

Chirped mirrors introduce a quadratic spectral phase; thereby the field amplitude of the output (compressed) pulse a_{out} is defined by

$$a_{out}(t) = F^{-1} \left(e^{-\frac{i\alpha\Omega^2}{2}} \cdot F(a(t, z = L)) \right) \quad (5)$$

where $\Omega = \omega - \omega_0$, α is the parameter of CM dispersion, and F and F^{-1} are the direct and inverse Fourier-transforms. The quantity α_{opt} designates the value of α at which the compressed pulse intensity I_{out} is maximal, hence, the intensity increase factor $F_i = I_{out}/I_{in}$ is maximal too. The numerical modeling (3-5) was performed for KDP and silica with the parameters given in Table 1. Values of B were varied from 0 to 20 by changing the input pulse intensity I_{in} . $B=10$ corresponds to an intensity of 0.79 TW/cm^2 for KDP and 1.18 TW/cm^2 for silica. Curves for $\alpha_{opt}(B)$ are plotted in fig. 1a. The dashed curves for $k_3=0$ are given for comparison. Analogous curves for $F_\tau = \tau_{in}/\tau_0$ and F_i at $\alpha = \alpha_{opt}$ are plotted in fig. 1 b,c.

Table 1. The parameters of numerical modeling

		KDP	Silica
L	mm	4	5
k_2	fs ² /mm	11.3	27.7
D		0.01	0.037
k_3	fs ³ /mm	123.7	106
T		0.0022	0.0023
n_2	10 ⁻¹⁶ cm/W	4.6	2.45
λ_0	nm	910	
T_F	fs	61	
N		20.1	

It is clear from fig. 1a that at large B the allowance for TOD in KDP (in contrast to silica) results in an increase in the absolute value of α_{opt} , which should be taken into consideration when planning experiments. In addition, with TOD taken into account, both F_τ and F_i become much larger for both KDP and silica. This is quite unexpected. Physically this is explained by the fact that at SPM the pulse acquires not only a positive quadratic spectral phase that is compensated by the negative quadratic dispersion of CMs, but also a negative cubic spectral phase that is partially compensated by the positive cubic dispersion of the medium. As the values of T are identical for KDP and silica (see Table 1), the TOD impact of these media is approximately the same (see fig.1 a-c).

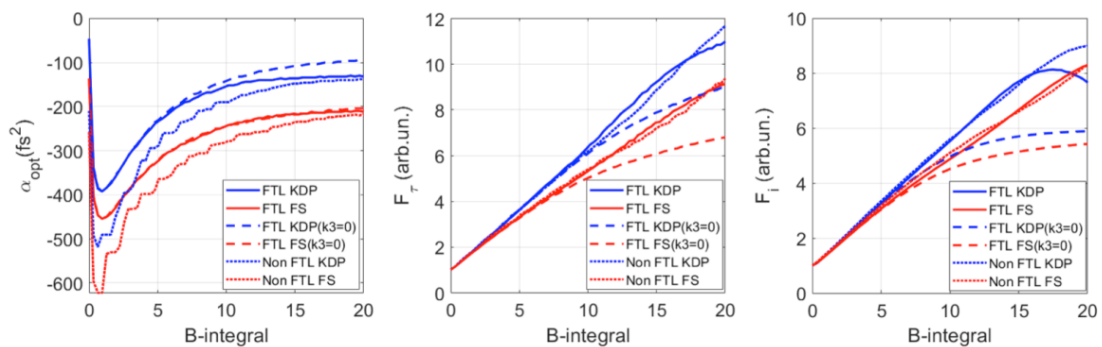


Fig.1 Curves for $\alpha_{opt}(B)$ (a), $F_\tau(B)$ (b), and $F_i(B)$ (c) for $\alpha = \alpha_{opt}$ for KDP (blue) and silica (red): FTL-pulse at $k_3 \neq 0$ (solid curves) and $k_3 = 0$ (dashed curves); non-Gaussian FTL-pulse, the spectrum and ACF of which are presented in fig. 3a (dotted curves).

On the basis of the above theoretical studies, we have developed a prototype of a pulse compressor and performed the corresponding experiments.

Experiments with the prototype

The schematic diagram of the prototype is shown in fig. 2. After reflection from the last diffraction grating of the compressor, the PEARL laser beam (central wavelength of about 910 nm) with a pulse energy of up to



18 J, a duration of 55-67 fs, and a diameter of 18 cm propagated 2.5 meters in free space for self-filtering. After that, the beam was propagated in a 4-mm thick home-made KDP crystal with angles of optical axes $\theta=\phi=0$. The output surface had an anti-reflecting coating. We used the reflection from the input uncoated surface to measure the spectrum and the autocorrelation function (ACF) of the input pulse. The measurements were made for a small part of the beam with a diameter of 1 cm. After free propagation over a distance of 6 m, the beam was reflected from CMs with a diameter of 20 cm manufactured by UltraFast Innovations GmbH (reflection coefficient >99%, bandwidth >200 nm). We used mirrors with sum dispersion $\alpha=-100 \text{ fs}^2$, -200 fs^2 , and -250 fs^2 . Besides, in the experiments with $\alpha=-200 \text{ fs}^2$ and -250 fs^2 we placed a 1-mm thick silica plate before the autocorrelator to introduce additional dispersion $\alpha=+28 \text{ fs}^2$, which is equivalent to the sum CMs dispersion $\alpha=-172 \text{ fs}^2$ and -222 fs^2 , respectively.

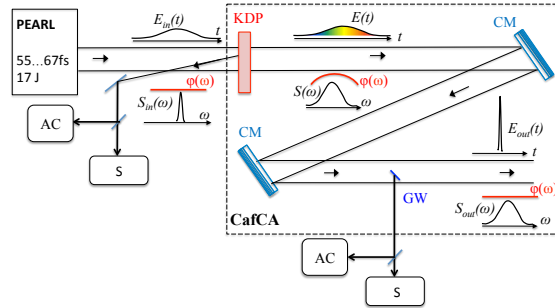


Fig.2. Schematic of the prototype. CM – chirped mirrors, GW – small-aperture glass wedge, AC – autocorrelators, S – spectrometers.

To measure the parameters of the output (compressed) pulse, a glass wedge (GW) with an aperture of 1x2 cm and a mat back surface was placed in the beam path. The beam reflected from the first surface of the wedge was directed to the spectrometer and the autocorrelator. The position of the wedge within the beam aperture corresponded to the place where the ACF and the spectrum of the input beam were measured, which made it possible to measure the characteristics of the input and output pulses in a single shot. We used 1.42 as a decorrelation factor to calculate the pulse duration from the autocorrelation function.

Typical measurement results are presented in fig. 3 for two shots at $\alpha=-200 \text{ fs}^2$. The output pulse spectra have characteristic narrow peaks arising because the input pulses are not FTL.

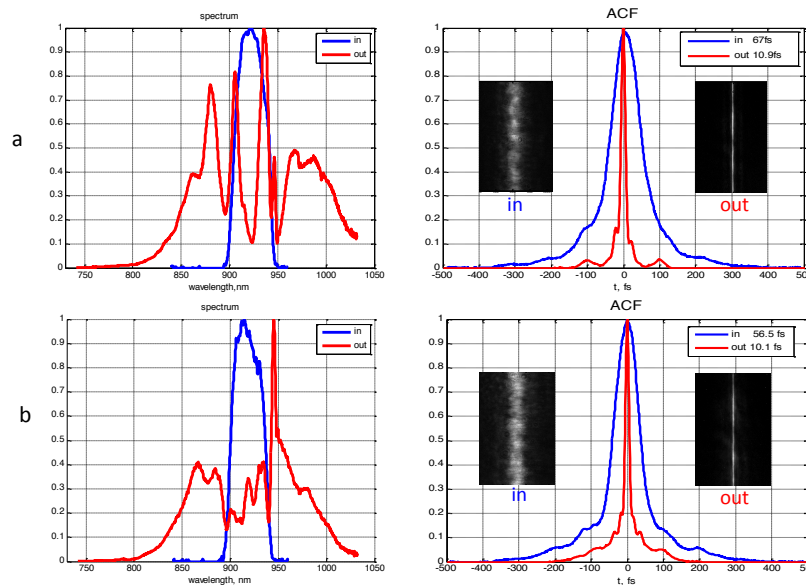


Fig.3. Measured input (blue) and output (red) spectra and ACF for two typical shots: $B=13$, $\tau_{in}=67 \text{ fs}$, $\tau_{out} = 10.9 \text{ fs}$ (a) and $B=14$, $\tau_{in}=57 \text{ fs}$, $\tau_{out} = 10.1 \text{ fs}$ (b).

Note that the measured output pulse spectrum is bounded at the longwave side by the spectrometer bandwidth (1030 nm).

An optimal value of CMs dispersion α_{opt} depends on B (see fig. 1a). The curves for the minimal duration of a compressed pulse τ_{out} as a function of α for two ranges $B=5...9$ and $B=11...19$ are plotted in fig. 4.



Analogous curves for 5-mm thick and 3-mm thick silica are also presented in this figure. Note that these are qualitative data, as a different number of shots was made for different values of α . Nevertheless, some conclusions follow from fig. 4.

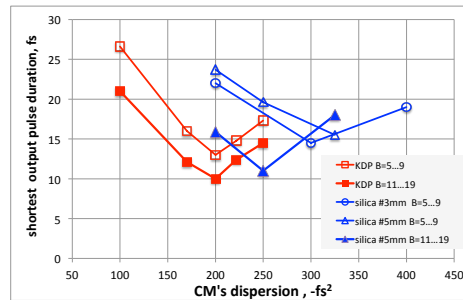


Fig.4. Experimental minimal compressed pulse duration τ_{out} for KDP ($L=4$ mm), silica ($L=5$ mm), and silica ($L=3$ mm [14, 19]) for two ranges of B value. The curves are plotted to make the figure more illustrative.

First, the value of α_{opt} decreases with a decrease in the parameter D : α_{opt} is maximal for 5-mm thick silica ($D=0.037$ at $\tau_{in}=61$ fs) and minimal for KDP ($D=0.01$ at $\tau_{in}=61$ fs). The difference is not very large for large values of B , but is significant for small B . This fully agrees with fig. 1a. Second, the absolute values of α_{opt} obtained experimentally are larger than those predicted theoretically (fig. 1 a). The reason is that the pulse used in experiments was not an FTL one. The absolute value of α_{opt} for such pulses is much larger than for FTL. To illustrate this fact we presented in fig. 1a an $\alpha_{opt}(B)$ curve for a KDP crystal for the case when the input pulse has the spectrum and ACF shown in fig. 3a: the dotted blue curve is lower than the solid curve. Third, from the viewpoint of minimal pulse duration, KDP, although slightly, is preferable to silica: 10 fs vs 11 fs at large values of B and 13 fs vs 16 fs at small B . This also agrees with the results of numerical modeling (see fig. 1).

The experimental data for $\tau_{in}=55...67$ fs obtained at $\alpha=-200$ fs² are presented in fig. 5. The peak power P_{out} for a compressed pulse with $\tau_{out}=10$ fs was 1.5 PW (we took into account the 20% losses associated with a lower intensity at the beam periphery and the respective larger τ_{out}). Despite the spread in the values in fig. 5, we can claim that at $\alpha=-200$ fs² there exists an optimal value of the B -integral (on the order of 15) at which τ_{out} is minimal and F_τ is maximal. With a further increase in B , the input pulse spectrum is broadened but, despite this fact, τ_{out} increases as $|\alpha_{opt}|$ is already less than 200 fs², i.e. CMs have redundant dispersion, as a result of which the output pulse is negatively chirped. At the same time, fig. 5 demonstrates that in a wide range of B -integral values from 11 to 19, for the same CMs set ($\alpha=-200$ fs²), all the shots are within the interval of τ_{out} from 9.3 fs to 13.6 fs and F_τ from 4.6 to 7. From the practical point of view, this spread is not very large and can be made even less if the input pulse has more stable duration and spectral phase.

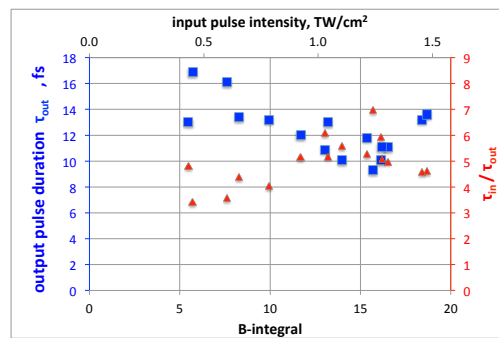


Fig.5. Output pulse duration τ_{out} (blue) and pulse compression factor $F_\tau=\tau_{in}/\tau_{out}$ (red) at $\alpha=-200$ fs²; $\tau_{in}=55...67$ fs.

Thus, we have experimentally demonstrated that KDP can give results not worse ($\tau_{in}/\tau_{out}>6$), and even a little better ($\tau_{out}=10$ fs) than those we have recently obtained with silica, with the superiority of KDP being still more pronounced for small B -integrals ($B=5...9$) (fig. 4). In addition, KDP has a number of other advantages. First, for KDP the α_{opt} values are smaller (figs. 1 a and 4). This allows a smaller number of mirrors to be used or the same number of mirrors but with lower dispersion, which are easier to produce. Second, for KDP the value of α_{opt} changes less with the variation of the B -integral (fig. 4). This makes it possible to use one set of CMs for a wide range of intensities, as demonstrated in fig. 5. Third, KDP anisotropy enables controlling linear and nonlinear properties of the material by choosing crystal orientation that is determined by the angles θ and ϕ .

Like in any uniaxial crystal, the linear refractive index (and, hence, k_2 and k_3) of an ordinary wave depends neither on θ nor on ϕ . However, similarly to any tetragonal crystal of $\bar{4}22$ symmetry, n_2 does not depend on θ , but is dependent on ϕ , and n_2 maxima and minima are, respectively, at $\phi=0+\pi m/2$ and $\phi=\pi/4+\pi m/2$ (m is the integer). Thus, for example, by rotating a z-cut crystal ($\theta=0$) around the z axis it is possible to continuously change the B-integral by about a factor of 1.5: $n_2(\theta=0, \phi=0)=4.6 \times 10^{-16} \text{ cm}^2/\text{W}$, and $n_2(\theta=0, \phi=\pi/4)=3.3 \times 10^{-16} \text{ cm}^2/\text{W}$. Still more opportunities are provided by an extraordinary wave for which k_2 and k_3 depend on θ , and n_2 depends on both, θ and ϕ . The functions $k_2(\theta)$ and $k_3(\theta)$ can be readily obtained from the known expression for $n_e(\theta)$ and from the Sellmeier equations. Thus, for an extraordinary wave, dispersion and nonlinearity can be controlled independently by varying θ and ϕ , respectively. Note that it is also possible to use a KDP crystal isomorph – a DKDP crystal whose dispersion strongly differs from KDP dispersion.

Conclusion

In our studies of the nonlinear compression of high-power laser pulses (TFC, CafCA, post-compression) after SPM in a KDP crystal we have obtained the pulse compression factor $\tau_{in}/\tau_{out}>6$ with the compressed pulse duration $\tau_{out}=10$ fs, which corresponds to a peak power of 1.5 PW. 10 fs is the shortest duration of all present-day petawatt lasers worldwide. It is important to note that the experiments were carried out for the B-integral values from 5 to 19, with no damage of the optical elements, which indicates that small-scale self-focusing is insignificant. Analogous results were recently obtained by our team using silica. However, as compared to silica, KDP has several advantages: (i) a larger pulse compression factor τ_{in}/τ_{out} , especially for $B=5\dots 9$; (ii) smaller absolute values of CMs dispersion α_{opt} ; (iii) smaller changes in α_{opt} with the variation of the B-integral; and (iv) a possibility to control both linear and nonlinear properties of the medium by choosing the orientation of the crystal's optical axis and the radiation polarization.

Taking into account the obtained results and the undoubted merits of nonlinear compression (simplicity, low cost, negligible pulse energy losses, and applicability to any high-power laser), we predict further development of this approach toward multi-PW power and single cycle pulse duration simultaneously.

Research team

The prototype of the SPM-based pulse compressor was developed by the following IAP RAS researchers: Efim Khazanov, Andrey Shaykin, Vladislav Ginzburg, Ivan Yakovlev, Alexey Kuzmin, Sergey Stukachev.

